ELSEVIER

Process Biochemistry 41 (2006) 2050–2057

Process Biochemistry

www.elsevier.com/locate/procbio

Nonlinear dynamic partial least squares modeling of a full-scale biological wastewater treatment plant

Dae Sung Lee [a], Min Woo Lee [a], Seung Han Woo [b], Young-Ju Kim [c], Jong Moon Park [a,*]

[a] *Advanced Environmental Biotechnology Research Center, Department of Chemical Engineering/ School of Environmental Science and Engineering, Pohang University of Science and Technology, San 31, Hyoja-dong, Pohang, Gyeongbuk 790-784, Republic of Korea*

[b] *Department of Chemical Engineering, Hanbat National University, San 16-1, Deokmyeong-dong, Yuseong-gu, Daejeon 305-719, Republic of Korea*

[c] *Department of Environmental Engineering, Kyungpook National University, Sankyuk-dong, Buk-gu, Daegu 702-701, Republic of Korea*

Received 11 December 2005; received in revised form 2 May 2006; accepted 4 May 2006

Abstract

Partial least squares (PLS) has been extensively used in process monitoring and modeling to deal with many, noisy, and collinear variables. However, the conventional linear PLS approach may be not effective due to the fundamental inability of linear regression techniques to account for nonlinearity and dynamics in most chemical and biological processes. A hybrid approach, by combining a nonlinear PLS approach with a dynamic modeling method, is potentially very efficient for obtaining more accurate prediction of nonlinear process dynamics. In this study, neural network PLS (NNPLS) were combined with finite impulse response (FIR) and auto-regressive with exogenous (ARX) inputs to model a full-scale biological wastewater treatment plant. It is shown that NNPLS with ARX inputs is capable of modeling the dynamics of the nonlinear wastewater treatment plant and much improved prediction performance is achieved over the conventional linear PLS model.

Keywords: Multivariate statistical process control; Neural network; Partial least squares (PLS); Dynamic system; Nonlinear system; Wastewater treatment plant

1. Introduction

Recent advances in computer technology and instrumentation techniques enable us to collect large amounts of data from chemical and biological processes. With the increasing data dimensionality, multivariate statistical process control (MVSPC) has become very important and essential to extract the useful information from the measurement data for improving process performance and product quality. During the last decade, it has been successfully applied for monitoring and modeling of chemical/biological processes [1–5].

One of the most popular MVSPC techniques is partial least squares (PLS). PLS is a linear multivariate process identification method that projects the input-output data down into a latent space, extracting a number of principal factors with an orthogonal structure, while capturing most of the variance in the original data [6,7]. Linear PLS derives its usefulness from its ability to analyze data with strongly collinear, noisy and numerous variables in both the predictor matrix **X** and responses **Y** [8].

However, when applying the linear PLS to modeling real processes, there have been some difficulties in its practical applications since most real problems are inherently nonlinear and dynamic [9–11]. A number of methods have been proposed to integrate nonlinear features within the linear PLS framework to produce a nonlinear PLS algorithm. A quadratic PLS modeling method was proposed to fit the functional relation between each pair of latent scores by quadratic regression [12]. Neural networks were also incorporated into linear PLS to identify the relationship between the input and the output scores, while retaining the outer mapping framework of linear PLS algorithm [13,14]. In the neural network PLS (NNPLS), because only small size network is trained at one time, the over-parametrized problem of the direct neural network approach such as multi-layer perceptron is circumvented even when the training data are very sparse. In addition, NNPLS does not require any kind of functional expansion compared to functional-link neural networks [15].

The conventional PLS implicitly assumes that the measurements are time independent and suited for modeling

* Corresponding author. Tel.: +82 54 279 2275; fax: +82 54 279 8659.
E-mail address: jmpark@postech.ac.kr (J.M. Park).

1359-5113/$ – see front matter
doi:10.1016/j.procbio.2006.05.006

steady-state processes. Typically, most of biological wastewater treatment plants are in dynamic state, with various events occurring such as hydraulic changes, composition variations, and equipment defects. Data from these processes are not only cross-correlated but also auto-correlated. Therefore, it is required to incorporate dynamic features of the process and to take into account time related variations of the process of interest. By simply augmenting a relatively large number of lagged values of the input variables in the input data matrix, called the finite impulse response (FIR) and including lagged values of both the inputs and the outputs in the input data matrix, called the auto-regressive with exogenous (ARX) inputs representations, dynamic relations can be modeled [16–18].

In the application investigated here, the NNPLS methodology is extended to enable the modeling of dynamic processes. By combining a static NNPLS with FIR and ARX model structure, nonlinear dynamic processes can be effectively modeled. The proposed methods were applied to a full-scale biological wastewater treatment plant and the modeling capabilities of these approaches were assessed through structured comparisons based on their prediction accuracy and performance characteristics.

2. Materials and methods

2.1. Domestic wastewater treatment plant

The full-scale biological wastewater treatment plant in Korea is a conventional activated sludge unit as shown in Fig. 1. It was designed for removal of organic matter from domestic wastewaters of nearby city in total 900,000 PE (persons equivalent). The removal of organic matter is accomplished in a biological system which consists of 24 primary clarifiers, 12 activated sludge lines, and 24 secondary clarifiers. The hydraulic retention time for primary clarifiers and aeration tanks were 2.7 and 7.9 h, respectively. The treatment efficiency is determined as the removal efficiency of total nitrogen, total phosphorus and total COD. Table 1 lists the available measurements from the plant along with their means and standard deviations. All samples were analyzed according to the Standard Methods [19]. Since the measurements were performed with different sampling intervals, the daily mean values for each variable were used in the data analysis. On-line measurements (temperature, flowrate, pH, and DO) were obtained at least once per hour. Some off-line analysis (COD, TN, and TP) were routinely performed twice a day but others (BOD, SS, SVI, and MLSS) once a day. All off-line analyses were repeated three times and their corresponding mean values were used for the model development. The process data used in modeling were routinely measured data and the investigation period was 12 months to cover the relevant information of the seasonal fluctuation.

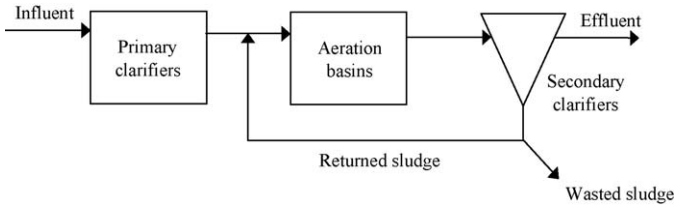

Fig. 1. Schematic diagram of the full-scale biological wastewater treatment plant.

2.2. Partial least squares

PLS reduces the dimension of the predictor variables **X** by extracting factors or latent variables which are correlated with responses **Y** while capturing a large amount of the variations in **X**. This means that PLS maximizes the covariance

Table 1
Measured variables at the full-scale biological wastewater treatment plant

No.	Variable	Symbol	Unit	Mean	Standard deviation	Skewness	Kurtosis
Influent							
1	Temperature	T_I	°C	17.0	4.8	−0.01	1.76
2	Flowrate	Q_I	m^3/day ($\times 10^3$)	400.5	72.7	1.82	7.15
3	pH	pH_I		7.1	0.1	0.21	1.99
4	BOD	BOD_I	mg/l	164.6	13.6	0.84	3.67
5	COD	COD_I	mg/l	206.0	63.8	0.60	2.94
6	SS	SS_I	mg/l	274.4	85.8	1.87	6.38
Primary clarifiers							
7	BOD	BOD_P	mg/l	65.2	12.6	0.10	3.66
8	COD	COD_P	mg/l	88.7	16.6	−0.02	3.18
9	SS	SS_P	mg/l	59.3	14.0	1.09	3.78
10	Total nitrogen	TN_P	mg/l	21.1	4.6	0.49	4.05
11	Total phosphorus	TP_P	mg/l	2.1	0.6	1.03	3.12
Aeration tanks							
12	MLSS	$MLSS_A$	mg/l ($\times 10^3$)	1.7	0.3	0.17	4.33
13	DO	DO_A	mg/l	2.6	1.4	0.50	2.44
14	Air flowrate	Q_{AIR}	m^3/day ($\times 10^6$)	1.5	0.1	0.92	4.04
15	SVI	SVI_A		201.0	75.6	0.86	3.04
16	Recycle flowrate	Q_R	m^3/day ($\times 10^3$)	198.0	24.0	0.28	1.78
17	Returned MLSS	$MLSS_R$	mg/l ($\times 10^3$)	5.1	1.1	0.78	3.76
18	Wastage flowrate	Q_W	m^3/day ($\times 10^3$)	6.0	1.3	−1.25	4.78
Effluent							
19	COD	COD_E	mg/l	14.0	2.2	−0.49	2.85
20	Total nitrogen	TN_E	mg/l	13.8	2.6	1.45	5.57
21	Total phosphorus	TP_E	mg/l	1.2	0.4	1.60	6.81

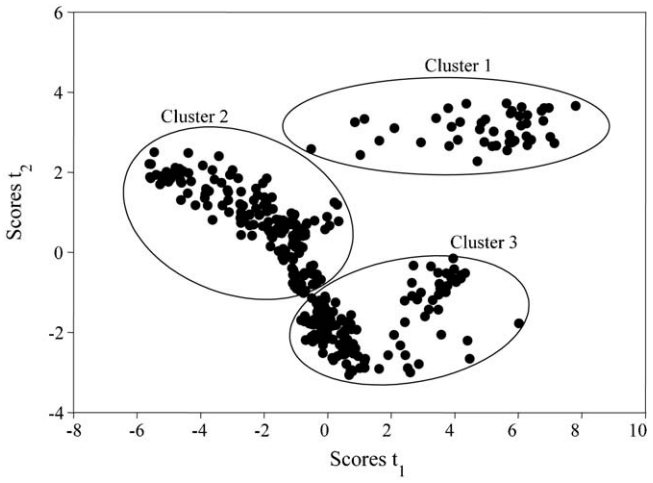

Fig. 2. PLS scores plot of all the operation data sets.

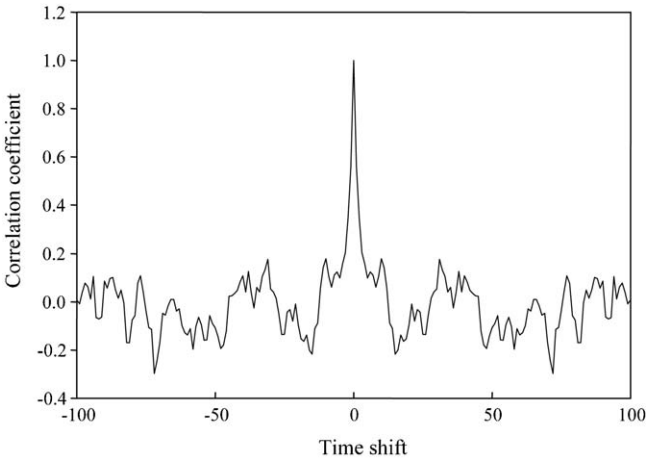

Fig. 3. Linear PLS: residuals auto-correlation coefficients.

Table 2
Cumulative variance captured (%) explained by linear PLS models

Principal component	Linear PLS		PLS-FIR		PLS-ARX	
	X	**Y**	**X**	**Y**	**X**	**Y**
1	49.45	71.47	49.07	73.99	51.22	74.34
2	67.50	78.17	66.49	78.34	67.03	81.18
3	75.20	81.05	73.17	81.58	74.34	84.54
4	79.81	83.27	77.85	84.70	78.48	87.15
5	83.66	84.60	80.50	85.18	80.95	88.40

between matrices **X** and **Y**. In PLS, the scaled matrices **X** and **Y** are decomposed into score vectors (**t** and **u**), loading vectors (**p** and **q**) and residual error matrices (**E** and **F**):

$$\mathbf{X} = \sum_{i=1}^{a} \mathbf{t}_i \mathbf{p}_i^T + \mathbf{E}$$
$$\mathbf{Y} = \sum_{i=1}^{a} \mathbf{u}_i \mathbf{q}_i^T + \mathbf{F} \quad (1)$$

where a is the number of latent variables. In an inner relation the score vector **t** is linearly regressed against the score vector **u**.

$$\mathbf{u}_i = b_i \mathbf{t}_i + h_i \quad (2)$$

where b is a regression coefficient which is determined by minimizing the residual h. There are several algorithms to calculate the PLS model parameters. In this work, the nonlinear iterative partial least squares (NIPALS) algorithm was used with the exchange of scores [6]. It is crucial to determine the optimal number of latent variables and cross-validation is a practical and reliable way to test the predictive significance of each PLS component.

2.3. Neural network partial least squares

In order to capture nonlinear structures between the predictor block and the responses, PLS model can be extended to nonlinear models. Major approaches have been to incorporate nonlinear functions within the linear PLS framework. Neural network PLS (NNPLS) is an integration of neural networks with PLS to model nonlinear processes with input collinearity [12]. The input and output variables are projected onto the latent space to remove collinearity and then

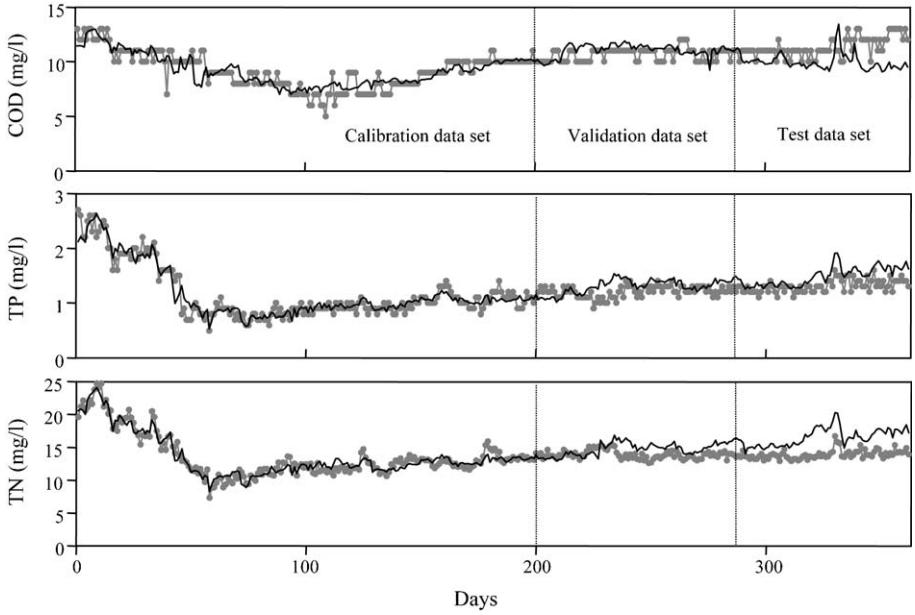

Fig. 4. Linear PLS model's performance (grey dotted line: measured, solid line: predicted).

each latent variable pair is mapped with a single-input-single-output (SISO) neural network as follows:

$$u_i = \boldsymbol{N}(t_i) + \boldsymbol{v}_i \tag{3}$$

where $\boldsymbol{N}(\cdot)$ stands for the inner relation represented by a neural network and $\boldsymbol{v}$ is the residuals. NNPLS's major advantage is that it decomposes a multivariate regression problem into a number of univariate regressors so that it can circumvent the over-parameterization problem. The neural network is trained to capture the nonlinearity in the projected latent space. In this application, a feed-forward back-propagation neural network (FBNN) with sigmoid functions was used to identify the nonlinear inner regression models for each of the latent variables.

2.4. Dynamic modeling approaches

In this study, two discrete regression models such as the finite impulse response and the auto-regressive with exogenous inputs representations are investigated [16,17,20]. By including lagged values of the input variables and outputs variables in the input data matrix, process dynamics can be incorporated into PLS model. The advantage of these approaches is that steady-state PLS techniques can be used for the modeling of dynamic process. To build FIR model, the process input vector $\mathbf{x}(k)$ which compromises lagged input data values is defined as:

$$\boldsymbol{x}_{\mathrm{FIR}}(k) = [\boldsymbol{x}(k-1), \boldsymbol{x}(k-2), \cdots, \boldsymbol{x}(k-n_x)]^{\mathrm{T}} \tag{4}$$

and the input vector for the ARX model is formulated as:

$$\mathbf{x}_{\mathrm{ARX}}(k) = [\mathbf{y}(k-1), \mathbf{y}(k-2), \cdots, \mathbf{y}(k-n_y), \mathbf{x}(k-1), \mathbf{x}(k-2), \cdots, \mathbf{x}(k-n_x)]^{\mathrm{T}} \tag{5}$$

where $\mathbf{x}(k)$ and $\mathbf{y}(k)$ are the process input and output data vectors, and n_x and n_y are the time lags for the input and output variables, respectively. With these approaches, the PLS methods can be extended to dynamic modeling by using either $\mathbf{x}_{\mathrm{FIR}}(k)$ or $\mathbf{x}_{\mathrm{ARX}}(k)$ as input vectors.

2.5. Experiments

The first 18 variables in Table 1 were used as predictors $\mathbf{X}$ to explain three response variables $\mathbf{Y}$ ($\mathrm{COD_E}$, $\mathrm{TN_E}$ and $\mathrm{TP_E}$), which serve as the purification result of the WWTP. To pre-treat data prior to this application, the sensor values were validated using a fault identification and reconstruction approach [21].

Initially, the historical data from 365 days of operation were analyzed by the linear PLS to understand the spatial patterns among the variables and to extract useful information from the process data. Then a number of linear and nonlinear dynamic PLS regression models were evaluated to predict the response variables. The data sets were divided into three parts. The first 200 observations were used for the development of PLS and NNPLS models. The next 80 observations and the remaining 85 observations were used as validation and test data sets, respectively, in order to verify the proposed methods. Both PLS and NNPLS models were calculated for the auto-scaled calibration set. Cross-validation was used to determine the optimal number of latent variables. With the respective PLS models, the results of the validation stage enabled the different modeling approaches to be evaluated and compared. The performance of each model was evaluated in terms of the root-mean-square-error (RMSE) criterion. The RMSE performance index was defined as:

$$\mathrm{RMSE} = \sqrt{\frac{\sum (\hat{y} - y)^2}{n}} \tag{6}$$

where y is the measured values, $\hat{y}$ is the corresponding predicted values and n is the number of samples. All programs used in this work were implemented in MATLAB by using the PLS toolbox [22].

3. Results and discussion

3.1. Analysis of historical process data

Initially, the whole data set was analyzed by the linear PLS. By examining the behavior of the process data in the projection spaces defined by the small number of latent variables in the case of PLS, it is often possible to extract very useful information. Fig. 2 shows the score values of all the data sets in the first two latent variables. This score plot gives the overall representation of the process behavior. The data points appear to cluster into three distinct regions which corresponded to different operating conditions. According to a priori knowledge, it was known that the transitions between cluster 1 and cluster 2 were from the rainy summer conditions. Average annual rainfall in Korea was about 1280 mm and about 2/3 of this rainfall was concentrated during the rainy summer from June to September. During the rainy season, high amount of diluted wastewater inflow to the WWTP (even though a large part of the wastewater inflow was bypassed) was frequent

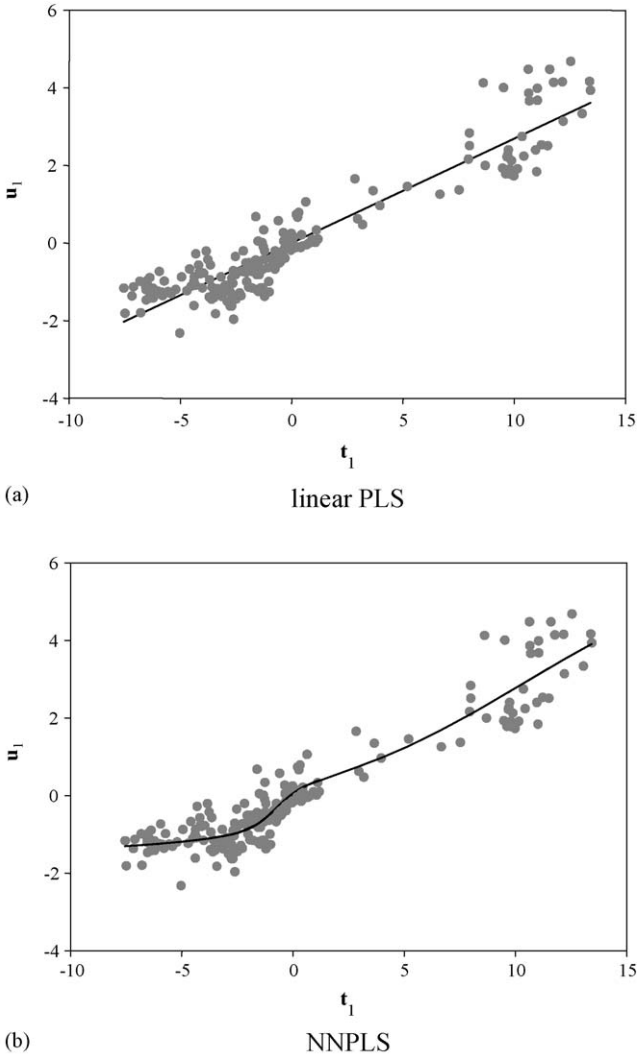

Fig. 5. Score plot of the first latent factor (light dot: data points, solid line: inner model).

Table 3
Cumulative variance captured (%) explained by NNPLS models

Principal component	NNPLS		NNPLS-FIR		NNPLS-ARX	
	X	**Y**	**X**	**Y**	**X**	**Y**
1	49.43	73.83	49.07	73.31	51.22	76.61
2	64.99	80.67	63.79	81.46	65.46	82.61
3	77.64	83.99	77.61	85.94	78.05	84.93
4	79.03	85.77	60.20	87.31	80.85	87.14
5	83.39	87.21	82.23	87.93	82.27	89.11

occurrence. This was a great disturbance to the WWTP and even significantly decreased the amount of microorganisms in the reactor. The scatter character of the plot also indicates that the operating data started from the left part of cluster 1 and gradually moved to cluster 2, and then the projected process data moved down to cluster 3. This implies that the WWTP operation was changing slowly and even switched to another operating state after disturbances such as the heavy rain conditions.

3.2. Linear PLS applications

A linear PLS model was built between the predictor variables and the response variables. The objective was to determine how well the linear model works and to compare the results to those of the dynamic and nonlinear models later. Based on the cross-validation results, five latent variables were included into the linear PLS model. It explained 84.60% of the variance of matrix **Y** and 83.66% of matrix **X** (Table 2). From the loading weights, we could find that previous values of the response variables themselves were the most important ones in predicting future values. However, in this application, it was difficult to identify the most important variables of the model

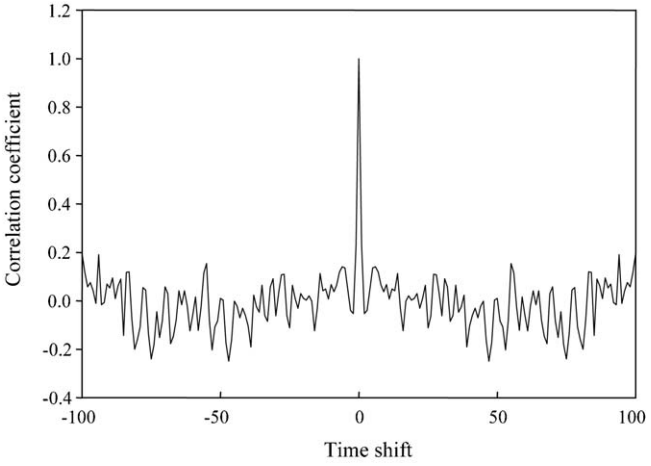

Fig. 6. NNPLS-ARX: residuals auto-correlation coefficients.

because their loadings vary considerably from one latent variable to another. The structure of the residual auto-correlation plot for the training data set is presented in Fig. 3. It indicates that there is a weak periodicity from slowly changing phenomena in the system. The simulation results of the linear PLS model are given in Fig. 4. This model predicted the dynamics of the wastewater treatment process with a relatively good accuracy for the calibration data set, but there was a significant mismatch between the model prediction and actual plant data in the later part of COD and TN profiles in the validation and test data sets. This exemplified the weakness of the linear multivariate regression model. Both FIR and ARX model structure were incorporated into the linear PLS. For the PLS-FIR model, the previous three samples of each predictor variables were used ($n_x = 3$). For the PLS-ARX model, the response variables at time $(k - 1)$ and $(k - 2)$ were used alongside the same process input variables used for the

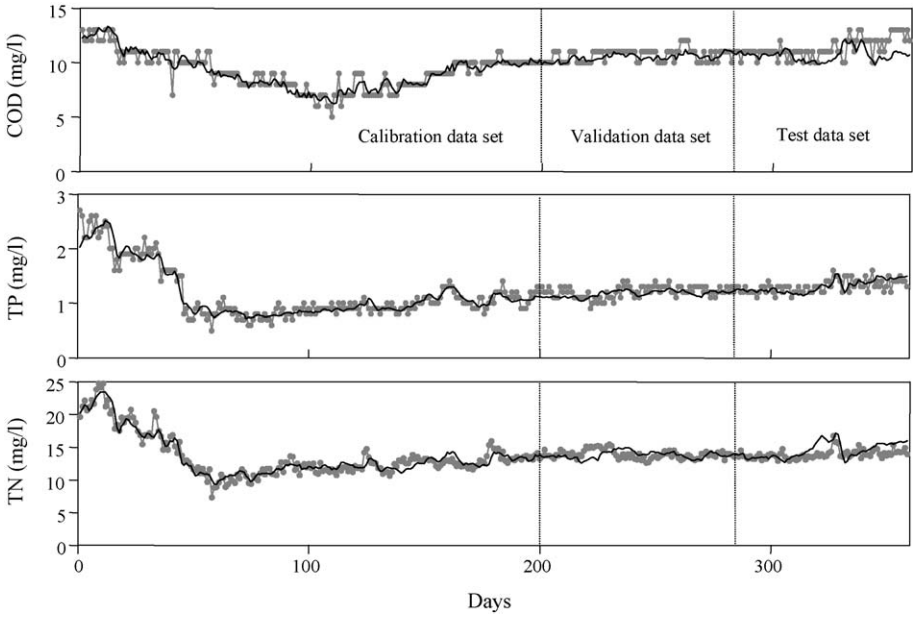

Fig. 7. NNPLS-ARX model's performance (grey dotted line: measured, solid line: predicted).

PLS-FIR model ($n_y = 2$). The time lags were determined by trial-and-error to minimize the RMSE of the validation data set. One-step-ahead predictions were chosen to enable the PLS models to be compared. The regression performance of the PLS-FIR and PLS-ARX models are also presented in Table 2. The improvement was seen when using an FIR model structure in contrast to the linear model structure, based on the captured variance of **Y**. Further improvement was obtained when using

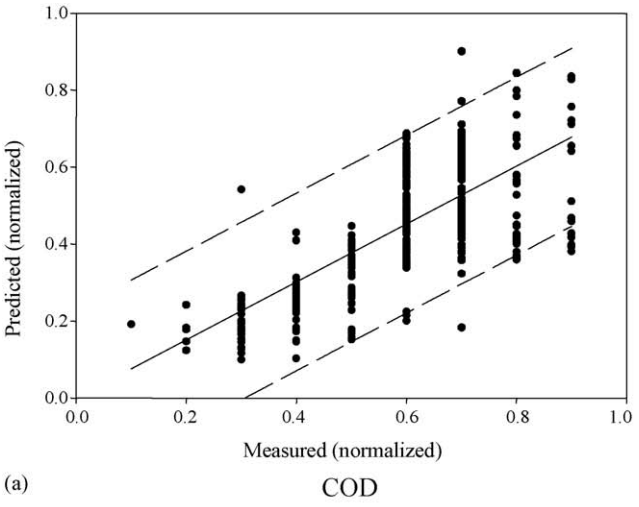

(a) COD

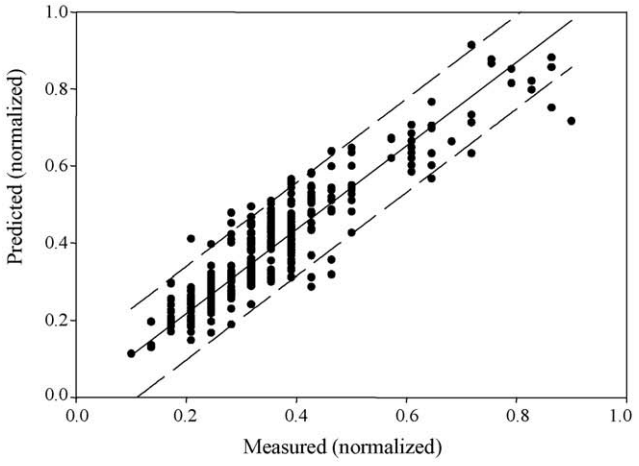

(b) TP

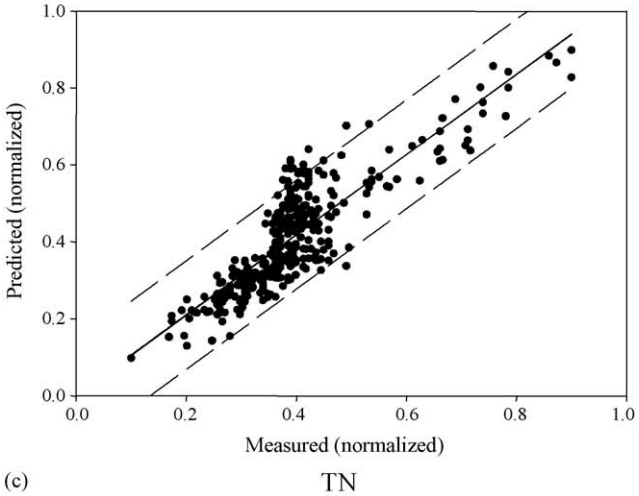

(c) TN

Fig. 8. Measured vs. predicted values by linear PLS model (long dash line: 95% prediction interval).

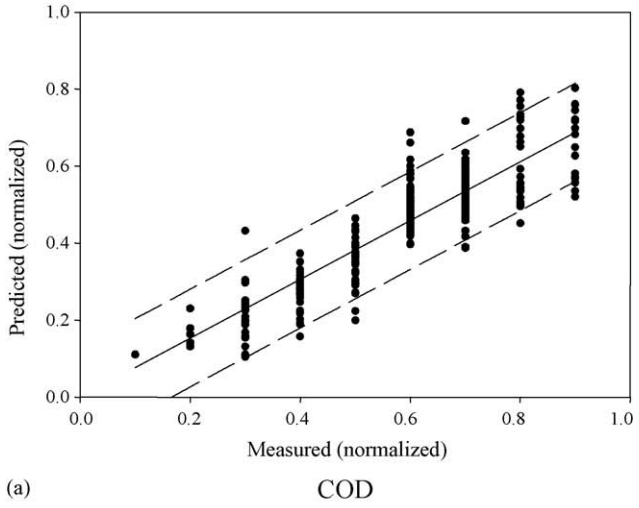

(a) COD

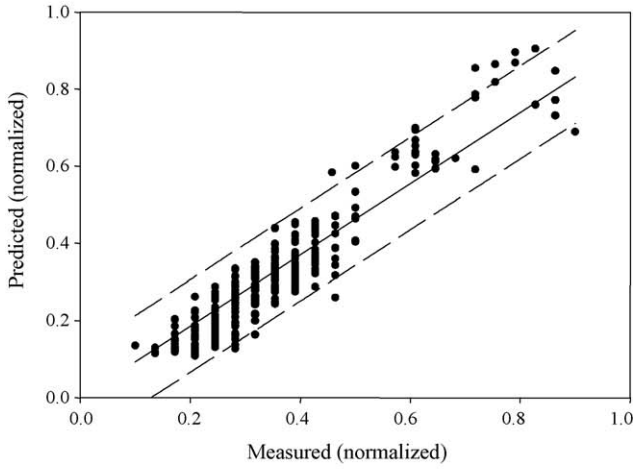

(b) TP

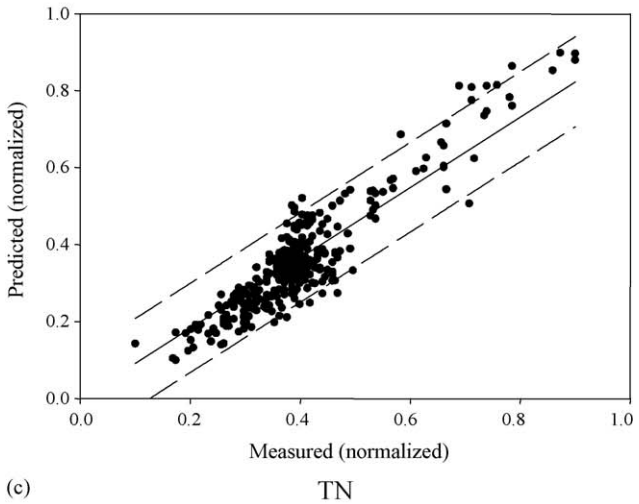

(c) TN

Fig. 9. Measured vs. predicted values by NNPLS-ARX model (long dash line: 95% prediction interval).

Table 4
Comparison of different models for the full-scale WWTP

Models	Structure	$RMSE_{calibration}$	$RMSE_{validation}$	$RMSE_{test}$	$R^2_{test,COD}$	$R^2_{test,Tp}$	$R^2_{test,TN}$
Linear PLS	Latent variables = 5	1.930	2.291	4.744	0.523	0.813	0.741
PLS-FIR	Latent variables = 5, $n_x = 3$	1.967	2.600	4.382	0.634	0.828	0.753
PLS-ARX	Latent variables = 5, $n_x = 3$, $n_y = 2$	1.794	2.208	3.960	0.677	0.840	0.767
NNPLS	SISO FBNN, factors = 5	1.915	2.047	3.848	0.604	0.825	0.751
NNPLS-FIR	SISO FBNN, $n_x = 3$, factors = 5	1.902	1.878	3.618	0.649	0.858	0.812
NNPLS-ARX	SISO FBNN, $n_x = 3$, $n_y = 2$, factors = 5	1.772	1.564	2.562	0.793	0.876	0.847

the ARX model structure in contrast to the FIR representation. Therefore, the predictor matrix including previous input and output values increase the amount of information, which enhances the predictive ability of the regression model.

3.3. Neural network PLS applications

In the application of the NNPLS modeling to this example, a feed-forward neural network with sigmoid functions was used to identify the nonlinear inner regression. The simplified cross-validation was used to determine the optimal number of factors [20]. Each factor is modeled using a SISO network. The neural network was trained to capture the nonlinearity in the projected latent space using a conjugate gradient optimization. The number of hidden units was also determined automatically by simplified cross-validation. The same data were also used to compare the PLS methods with the NNPLS models. Five latent variables were included into the NNPLS model, which then explained 83.39% of the variance of matrix **X** and 87.21% of matrix **Y** (Table 3). Fig. 5 shows the first principal inner relation between the **X** and **Y**-block from both the linear PLS and NNPLS models. Fig. 5(a) shows a very strong relationship and the linear PLS regression gives a best linear least-squares model. Fig. 5(b), when it is compared with Fig. 5(a), clearly shows how the NNPLS model captures the nonlinearity and thus outperforms the linear PLS model. By using the same time-lagged input matrix ($n_x = 3$, $n_y = 2$), both NNPLS-FIR and NNPLS-ARX models were developed. The regression performance of the dynamic models is also presented in Table 3. From the residual auto-correlation plots for the training data set as shown in Fig. 6, it indicates that the NNPLS-ARX model exhibits less periodical behaviors, compared to the linear PLS model (Fig. 3). Fig. 7 presents the regression results from the NNPLS-ARX model. It shows that the NNPLS-ARX gives much better prediction results than the linear PLS model (Fig. 4). Hence, not only is the NNPLS-ARX model able to model the nonlinearity of the full-scale WWTP, the dynamic structure of the model can capture the complex dynamics of the problem. The measured data versus the predicted values of COD, TP and TN concentrations from both the linear PLS and NNPLS-ARX model are shown in Figs. 8 and 9, respectively. These results consistently showed that the NNPLS-ARX model outperformed the linear PLS model.

Table 4 shows the RMSE and coefficient of multiple determination (R^2) values of six different modeling approaches. It can be observed that the prediction capabilities of the linear PLS approach improved when either nonlinear modeling method or dynamic input structures were employed. The overall performance of the NNPLS-ARX model is better in terms of both the RMSE and R^2 values than any other algorithms. The increased prediction performance of the NNPLS-ARX model can be explained by the fact that the full-scale WWTP, in this application, is an inherently nonlinear dynamic system with time-varying reactions of the micro-organisms and large variations in the incoming wastewater.

4. Conclusions

Although the conventional PLS modeling method gives a linear model from a lot of collinear measurements, it is not capable of modeling nonlinear and dynamic systems. By integrating a nonlinear NNPLS modeling algorithm with dynamic FIR and ARX framework, nonlinear dynamic systems can be modeled effectively. Application to a full-scale biological WWTP has shown that the NNPLS with ARX model representation gave the best prediction performance benefiting from the inclusion of a nonlinear inner mapping and dynamic input structure. However, in this application, the model's results should not be extrapolated without care as the validation and test data sets showed rather little dynamics. Since the developed model was derived from daily mean values, it might not be appropriate for control purposes. But it can give operators and process engineers a guideline that would allow them to arrive at the optimum operational strategy.

The methodology is fairly general and applicable to other biological WWTPs. As most full-scale domestic/industrial wastewater treatment plants have typically little detailed knowledge of the process or of its response to external disturbances, we believe that the proposed modeling strategy can be widely applied to complex and time-varying biological systems for development of cost-effective and reliable prediction models.

Acknowledgements

The work was financially supported by the ERC program of MOST/KOSEF (R11-2003-006-01001-1) through the Advanced Environmental Biotechnology Research Center at POSTECH. This work was also supported by the ET edu-innovation Project of Ministry of Environment in 2006.

Appendix A. Nomenclature

a	number of latent variables
ARX	auto-regressive with exogenous input
b	regression coefficient
COD	chemical oxygen demand (mg/l)
E	error matrix
F	error matrix
FBNN	feed-forward back-propagation neural network
FIR	finite impulse response
h	residuals
MVSPC	multivariate statistical process control
n	number of samples
n_x, n_y	time lag for the input and output variables
NNPLS	neural network partial least squares
p	loading vector
PE	persons equivalent
PLS	partial least squares
q	loading vector
RMSE	root-mean-square-error
t	score vector
TN	total nitrogen (mg/l)
TP	total phosphorus (mg/l)
u	score vector
$\boldsymbol{v}$	residuals
WWTP	wastewater treatment plant
x	input vector
X	predictor matrix
y	measured variable
$\hat{y}$	predicted value
Y	response matrix

References

[1] Lee DS, Jeon CO, Park JM, Chang KS. Hybrid neural network modelling of a full-scale industrial wastewater treatment process. Biotechnol Bioeng 2002;78:670–82.

[2] Lee DS, Park JM, Vanrolleghem PA. Adaptive multiscale principal component analysis for on-line monitoring of a sequencing batch reactor. J Biotechnol 2005;116:195–210.

[3] Lee DS, Vanrolleghem PA. Monitoring of a sequencing batch reactor using adaptive multiblock pricipal component analysis. Biotechnol Bioeng 2003;82(4):489–97.

[4] MacGregor JF, Kourti T. Statistical process control of multivariate processes. Control Eng Pract 1995;3:403–14.

[5] Wise BM, Gallagher NB. The process chemometrics approach to process monitoring and fault detection. J Proc Control 1996;6:329–48.

[6] Geladi P, Kowalski BR. Partial least-squares regression: a tutorial. Anal Chim Acta 1986;185:1–17.

[7] Wold S, Ruhe A, Wold H, Dunn WJ. The Collinearity problem in linear regression. The partial least squares approach to generalized inverse. SIAM J Sci Stat Comput 1984;3:735–43.

[8] Wold S, Sjöström M, Eriksson L. PLS-regression: a basic tool of chemometrics. Chemom Intell Lab Syst 2001;58:109–30.

[9] Baffi G, Martin EB, Morris AJ. Non-linear projection to latent structures revisited (the neural network PLS algorithm). Comput Chem Eng 1999;23:1293–307.

[10] Wang X, Kruger U, Lennox B. Recursive partial least squares algorithms for monitoring complex industrial processes. Cont Eng Practice 2003;11:613–32.

[11] Gallagher NB, Wise BM, Butler SW, White DD, Barna GG. Development and benchmarking of multivariate statistical process control tools for a semiconductor etch process: improving robustness through model updating. In: Proceedings of the ADCHEM 97. Banff, Canada; 1997. p. 78.

[12] Wold S, Kettaneh-Wold N, Skagerberg B. Nonlinear PLS modeling. Chemom Intell Lab Syst 1989;7:53–65.

[13] Lee DS, Vanrolleghem PA, Park JM. Parallel hybrid modeling methods for a full-scale cokes wastewater treatment plant. J Biotechnol 2005;115:317–28.

[14] Qin SJ, McAvoy TJ. Non-linear PLS modelling using neural networks. Comput Chem Eng 1992;16:379–91.

[15] Chen S, Billings SA. Neural network for nonlinear dynamic system modeling and identification. Int J Cont 1992;56:319–46.

[16] Baffi G, Martin EB, Morris AJ. Non-linear dynamic projection to latent structures modelling. Chemom Intell Lab Syst 2000;52:5–22.

[17] Qin SJ, McAvoy TJ. Nonlinear FIR modelling via a neural net PLS approach. Comput Chem Eng 1996;20(2):147–59.

[18] Ricker NL. The use of biased least-squares estimators for parameters in discrete-time pulse response models. Ind Eng Chem Res 1988;27:343–50.

[19] APHA. Standard methods for the examination of water and wastewater, 19th ed. Washington DC: American Public Health Association; 1995.

[20] Qin SJ. Partial least squares regression for recursive system identification. In: Proceedings of the 32nd Conference on Decision and Control. San Antonio, Texas; 1993. p. 2617.

[21] Dunia R, Oin SJ, Edgar TF, McAvoy TJ. Identification of faulty sensors using principal component analysis. AIChE J 1996;42:2797–812.

[22] Wise BM, Gallagher NB. PLS toolbox version 2. 1 for use with MATLAB™ Washington DC: Eigenvector Research; 2000.